INTERNATIONAL JOURNAL OF CLIMATOLOGY
Int. J. Climatol. **24**: 33–44 (2004)
Published online in Wiley InterScience (www.interscience.wiley.com). DOI: 10.1002/joc.984

CHANGES IN THE SUB-DECADAL COVARIABILITY BETWEEN NORTHERN HEMISPHERE SNOW COVER AND THE GENERAL CIRCULATION OF THE ATMOSPHERE

KAZUYUKI SAITO,[a,*] TETSUZO YASUNARI[a,b] and JUDAH COHEN[c]

[a] *Frontier Research System for Global Change, 3173-25 Showa-machi Kanazawa-ku, Yokohama City, Kanagawa, 236-0001, Japan*
[b] *Hydrospheric Atmospheric Research Center, Nagoya University, Furo-cho, Chigusa-ku, Nagoya City, Aichi, 464-8601, Japan*
[c] *Atmospheric and Environmental Research, Inc., Lexington, MA 02421, USA*

Received 23 June 2003
Revised 21 October 2003
Accepted 21 October 2003

ABSTRACT

Details of the sub-decadal covariability relationship between continental snow cover extent anomalies and the dominant mode of atmospheric variability, referred to as the Arctic oscillation (AO) or North Atlantic oscillation (NAO), for the period 1971–2001 are explored. On the seasonal time scale, the winter AO is found to be significantly correlated with the preceding autumn Eurasian snow cover (SNC_{EUR}) throughout the period observed. Consistent with this finding, SNC_{EUR} variability led the AO variability on the sub-decadal time scale in the early half of the record. However, starting in the mid 1980s, the AO and SNC_{EUR} vary in phase. Analyses of the seasonal relationship and persistence of snow and atmospheric variables illustrate a phase shift in the sub-decadal variability between the AO and SNC_{EUR} due to the loss of autumn–winter SNC_{EUR} autocorrelation replaced by a significant winter–spring persistence and the emergence of a concurrent SNC_{EUR}–AO connection in winter and spring. Similar analysis shows that the sub-decadal NAO variation is mostly described by the fluctuation in summer North American snow cover. Copyright © 2004 Royal Meteorological Society.

KEY WORDS: Northern Hemisphere; snow–climate interaction; interannual variability; atmospheric general circulation; observational data analysis

1. INTRODUCTION

The dominant mode of Northern Hemisphere (NH) atmospheric variability, the North Atlantic oscillation (NAO) or Arctic oscillation (AO), is known to have significant spectral peak(s) at interannual and/or longer time scales (Marshall *et al*., 2001; Robertson, 2001). Feldstein (2002) demonstrated that the increased interannual variance of the dominant mode of atmospheric variability after the 1960s is larger than expected if it is solely driven by internal (intraseasonal) fluctuations of the atmosphere, suggesting coupling with other components of the climate system (hydro- and/or cryo-sphere) and/or forcings external to the system. Links and covariabilities of the interannual fluctuation of the dominant mode within the system have been found in sea-surface temperature, sea ice, and snow cover (e.g. Czaja and Frankignoul, 1998; Cohen and Entekhabi, 1999; Wang and Ikeda, 2000).

Saito and Cohen (2003) show that the dominant mode and continental snow cover have significant coherency at the sub-decadal (6–10 year) period, and that snow cover leads the atmosphere by several months. The results in that previous paper are, however, derived from analysis in the frequency domain and, therefore, do not provide a detailed profile in the temporal domain. In this article we report a more detailed description of

* Correspondence to: Kazuyuki Saito, Frontier Research System for Global Change, 3173-25 Showa-machi Kanazawa-ku, Yokohama City, Kanagawa, 236-0001, Japan; e-mail: ksaito@jamstec.go.jp

changes in the sub-decadal covariability between the continental snow cover extent and the dominant mode during the remotely sensed period. The identity of and the difference between the AO and NAO remain controversial. We use 'the dominant mode' as a general term to cover both; however, we will refer to AO and NAO variability individually in association with fluctuations with continental snow cover. Previous studies have shown (and we will also show) that Eurasian snow cover (SNC_{EUR}) is more closely related to the AO, and that North American snow (SNC_{NA}) is related to the NAO (Cohen and Entekhabi, 1999; Bojariu and Gimeno, 2003; Saito and Cohen, 2003; Saunders *et al*., 2003).

2. DATA AND RESULTS

We use monthly NAO and AO indices, as defined by Hurrell and van Loon (1997) and by Thompson and Wallace (1998) respectively. Continental snow cover areas for Eurasia and North America (excluding Greenland) are calculated from satellite observations and provided by the Snow Data Resource Center, Rutgers University Climate Lab (Robinson *et al*., 1993). We use National Centers for Environmental Prediction–National Center for Atmospheric Research reanalysis (Kalnay *et al*., 1996) for atmospheric variables. Surface temperatures are provided by the Climate Research Unit, University of East Anglia (Jones and Moberg, 2003), for land and by the Hadley Centre (Rayner *et al*., 2002) for ocean.

First, we look at 70–120 month period variation, bandpass-filtered by wavelet analysis with Mexican hat (Marr) wavelet (Torrence and Compo, 1998), of the monthly normalized series of the AO index and the Eurasian snow cover extent anomaly (SNC_{EUR}) from 1971 through to 2001 in Figure 1(a). The e-folding time for that period range corresponds to from 24.9 to 42.7 months, or about 2 to 3.5 years; both ends of the range are influenced by edge effects due to the finite length of the series analysed, and hence the amplitude is presumably reduced. The filtered AO and SNC_{EUR} show a distinct change in phase between the first and the second halves of the remotely sensed period delineated by the mid 1980s (Figure 1(a)). For the first half, SNC_{EUR} tends to lead the AO variability by several or more months, whereas for the second half the two series vary almost in phase.

Next we examine the season most representative of the observed SNC_{EUR} and AO sub-decadal variability. The two filtered time series shown in Figure 1(a), are presented in Figure 1(b) and (c) respectively, including a 3-year running mean (thin line) of detrended seasonal anomalies. Until the mid 1980s, for SNC_{EUR} it is the winter that best resembles the sub-decadal fluctuation, whereas in the later period the warm season (spring to autumn) accounts for more of the interannual variability (Figure 1(b)). For the AO, it is primarily winter (December to February; DJF) that represents most of the variation in the sub-decadal fluctuations through the period. Spring (March to May; MAM) variability only exhibits a strong relation with winter variability after the mid 1980s (Figure 1(c)).

A corresponding change between the two periods is found in the seasonal relation between SNC_{EUR} and the AO. Figure 2(a) shows the Spearman (rank) correlation of SNC_{EUR} between successive seasons for running 12-year periods. Rank correlation is used in this study to minimize outlier influence, although Pearson's linear method produces substantially the same results. The statistically significant autocorrelation between autumn (September to November; SON) and the following DJF SNC_{EUR} found in the earlier period is lost after the emergence of a significant DJF–MAM autocorrelation in the mid 1980s. A similar emergence of a significant DJF–MAM lagged cross-correlation is also observed between the DJF AO and the MAM SNC_{EUR}, and concurrent cross-correlation between the two variables in winter and spring is consistently seen throughout the entire period (Figure 2(b)).

3. DISCUSSION

The changes in the seasonal autocorrelation of SNC_{EUR} and its correlation with the AO, as indicated in Figure 2, may be responsible for the changes in the sub-decadal covariability shown in Figure 1(a). Given the above results, we present the following hypothesis to explain the difference in the covariability between

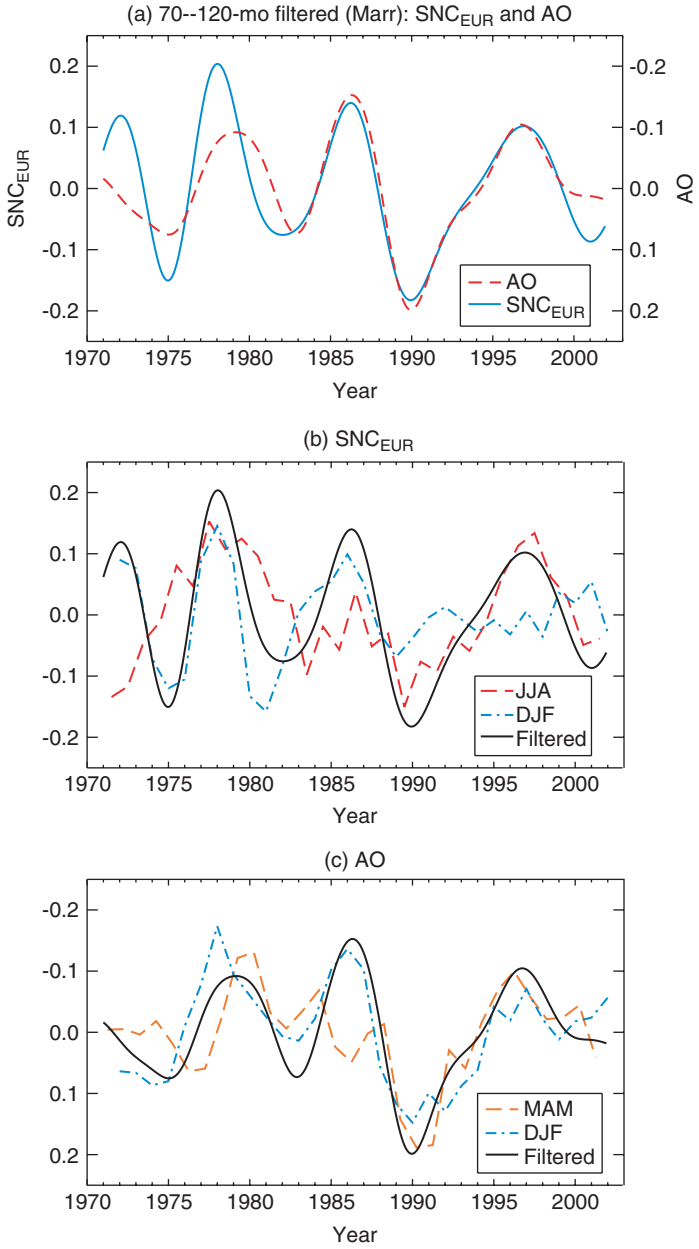

Figure 1. (a) 70–120 month bandpass-filtered monthly anomaly time series of Eurasian snow cover (solid; SNC_{EUR}) and the AO (dashed; scale at right). (b) 70–120 month bandpass-filtered monthly anomaly (thick) and 3-year running mean of detrended JJA (long-dashed) and DJF (dash-dotted) seasonal anomaly of SNC_{EUR}. (c) As (b), but for the AO (thick) and its MAM (dashed) and DJF (dash-dotted) seasonal anomaly. This figure is available in colour online at http://www.interscience.wiley.com/ijoc

SNC_{EUR} anomalies and the AO for the two periods. For the earlier period, the autumn SNC_{EUR} persisted into winter while also leading the winter AO variability (Figure 2(a) and (b)). Also, during the earlier period, the spring SNC_{EUR} had only a weak relation with the winter AO and winter SNC_{EUR} (Figure 2(a) and (b)). This resulted in SNC_{EUR} leading the AO by several or more months through their mutual oscillations (Figure 1(a)). For the later period, although autumn SNC_{EUR} still leads the winter AO, it is no longer correlated strongly with the winter SNC_{EUR}; rather, winter SNC_{EUR} exhibits strong persistence into the spring. Spring SNC_{EUR} is

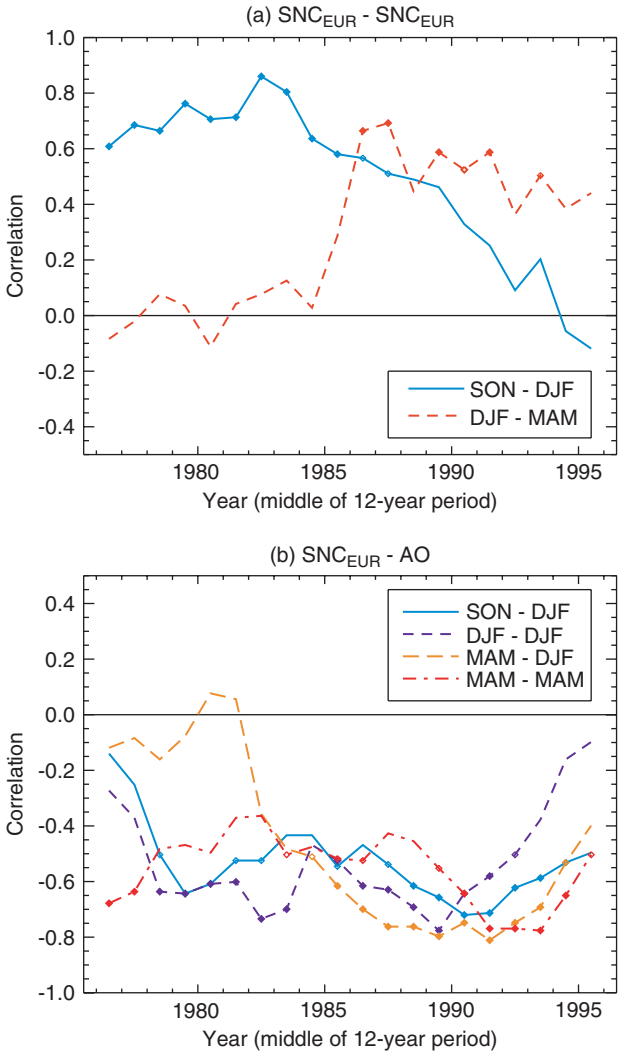

Figure 2. (a) Rank correlation of SNC_{EUR} between autumn and winter (solid) and winter and spring (dashed) for running 12-year period, plotted at the middle of each period. Filled (open) diamonds denote significant at 5% (10%) confidence level. (b) As (a), but for the AO and SNC_{EUR} between different combination of seasons. This figure is available in colour online at http://www.interscience.wiley.com/ijoc

now strongly connected to the winter and spring AO (Figure 2(a) and (b)); therefore, sub-decadal variability for both climate variables is now dominated by winter to spring variations (Figure 1(b) and (c)), resulting in their variation in phase (Figure 1(a)).

Still an important question remains: Why did the persistence of the SNC_{EUR} and winter AO–spring SNC_{EUR} relation change between the two periods whereas the autumn SNC_{EUR}–winter AO relationship held throughout the entire period despite small-amplitude fluctuations (Figure 2(b))?

We select two 12-year periods, i.e. 1974–85, and 1986–97, for further analysis and present selected environmental fields for each period in an effort to illustrate and explain the observed change and difference between the periods delineated by the mid 1980s. Figure 3 shows composite differences between five extreme years of each sign with respect to SON SNC_{EUR} to show the location and magnitude of maximum differences between both extremes. The month shown in the figure denotes the centre of a 1–2–1 weight applied to three adjacent months. The time series and environmental fields are detrended within a semi-period. Significance is tested using a *t*-test. Field significance is tested against a null distribution of areas of significant local

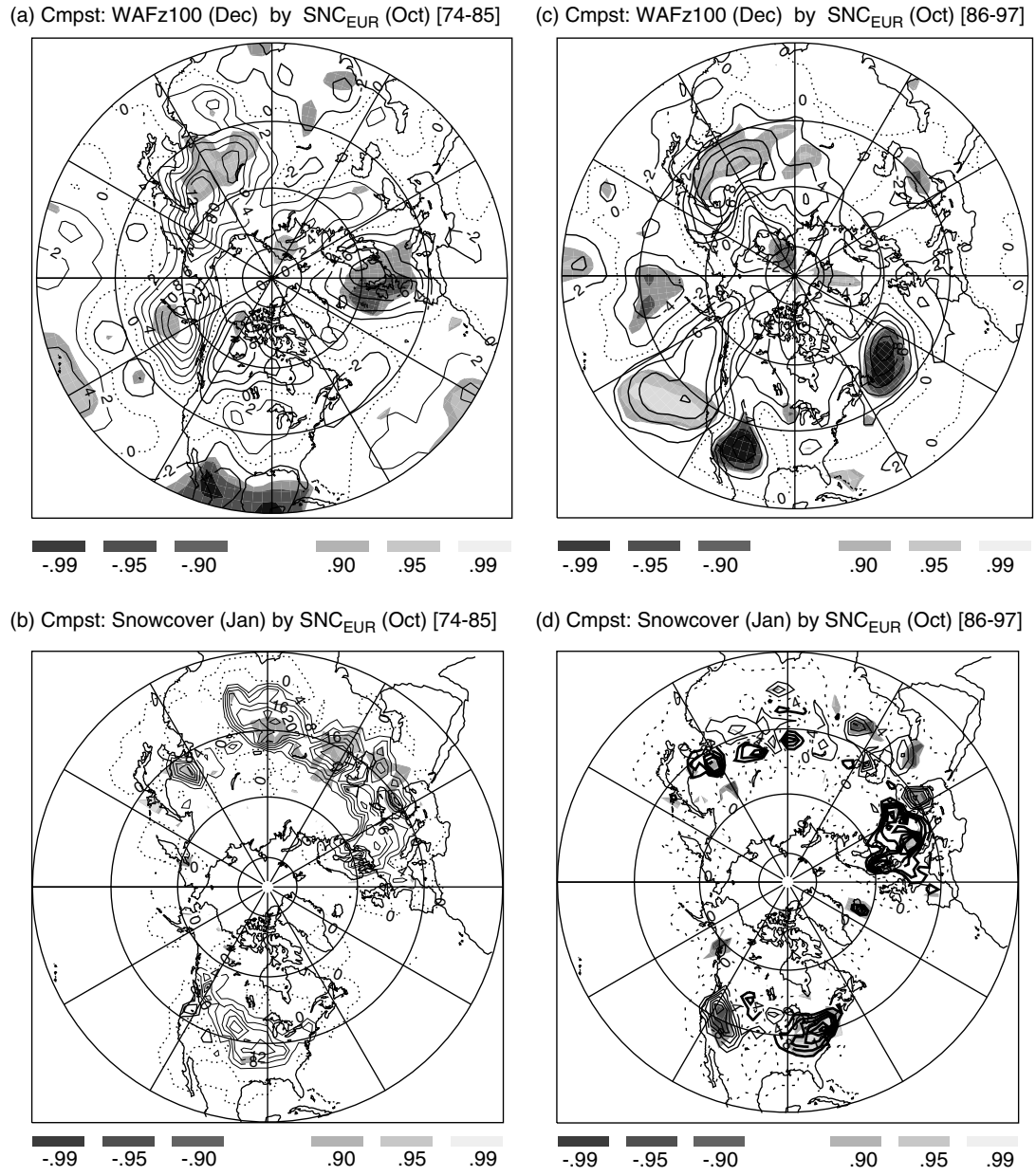

Figure 3. (a) Composite of December vertical WAF (WAF_z) at 100 hPa between five extensive and sparse October SNC_{EUR} for 1974–85. Contour interval is 2 m^2 s^{-2}, and positive (negative) values are contoured in thick (thin). Significance at 10, 5, 1% level in positive and negative directions is shown by grey-scale gradation. WAF_z field and SNC_{EUR} series are 1–2–1 weighted with those of adjacent months. (b) As (a) but for January snow cover. Contour interval is 4%. (c) As (a) and (d) as (b), except for the period 1986–97

correlation at the 5% significance level, which is constructed by the time series permutated in a random order. The domain is defined to include focused regions of each relationship. The results are summarized in Table I.

Previous studies have demonstrated that autumn SNC_{EUR} influences the winter AO by modulating the upward propagation of the stationary Rossby waves as diagnosed by the wave activity flux (Plumb, 1985; WAF_z), both with observational (Saito *et al*., 2001) and numerical modelling studies (Gong *et al*., 2003).

Table I. Results of field significance test. Percentage area of local significance denotes total areas of grid cells that show significant local correlation at 5% significance level within the domain

Figure no.	Figure part	Domain	Percentage area of local significance[a]
3	(a)	[80–180 °E, 40–65 °N]	7.38+
	(c)		7.96+
	(b)	[0–180 °E, 30–70 °N]	6.07*
	(d)		2.46
5	(a)	[0–360 °E, 30–85 °N]	17.3*
	(d)		21.1*
	(b)	[0–180 °E, 30–70 °N]	4.53
	(e)		19.2*
	(c)	[0–180 °E, 30–70 °N]	3.72
	(f)		6.56*

[a] +: within upper 10%; *: within upper 5%.

Changes to the atmospheric circulation, forced by anomalous SNC_{EUR}, are consistent with existing theories on troposphere–stratosphere coupling (Zhou *et al*., 2002). The upward WAF_z anomaly, field significant over northeastern Eurasia at 10% (Table I), is observed in late autumn–early winter for both periods. Although the location of the anomalous upward WAF_z does vary between the two semi-observational periods, both regions of anomalous flux lie within the major Siberian wave train of upward flux (Plumb, 1985), consistent with previously demonstrated results. Therefore, during both semi-periods, variations in autumn SNC_{EUR} are likely to initiate changes in the AO consistent with known troposphere–stratosphere coupling.

We next present snow-cover expansion from October through to January for both semi-periods by a composite difference of January snow cover with respect to October SNC_{EUR} (Figure 3(b) and (d)). SON–DJF persistence in the earlier semi-period is due to an organized, almost zonally uniform advance of snow cover. These areas cover most of the regions of 'active' snow-cover fluctuation, as shown in figure 3 of Clark *et al*. (1999). In contrast, during the latter period, no organized expansion is seen except for a limited region of central Europe. Clark *et al*. (1999) argue that the atmosphere controls the Eurasian snow cover extent during winter (DJF) and demonstrate that three teleconnection patterns have distinct and different regional forcing of the extent of Eurasian snow cover.

We define HA as the area-weighted mean of the normalized geopotential height anomaly Z north of 60 °N at each pressure level (Cohen *et al*., 2002). HA serves as an excellent proxy for the AO (see Figure 4(a)), yet it also captures the dominant regional variability of height anomaly at high latitudes, including the strength of the polar vortex at each pressure level. The monthly series of the AO, defined as the first principal component of the geopotential height anomaly field, and HA at the same pressure level have substantial coherency on monthly to sub-decadal time scales (not shown).

Differences in tropospheric persistence between the two periods are shown by HA_{500} (Figure 4(b)), i.e. HA defined at 500 hPa, which exhibits similar seasonal characteristics as SNC_{EUR} (Figure 2(a)). The 500 hPa level is chosen for display, but similar results are obtained for 700 hPa through to 200 hPa. Through composite analysis, HA_{500} variability in the earlier semi-period is found to relate to a pattern similar to the Eurasian Type 1 pattern (Barnston and Livezey, 1987; EU1) from autumn to winter in the pressure/height fields, and to anomalous surface temperature over northeastern Eurasia (not shown). Temperatures in this region are known to be more sensitive to the EU1 pattern than southwestern Eurasia (Clark *et al*., 1999). The strong autocorrelation in autumn–winter SNC_{EUR} before the mid 1980s may be due to the persistence of the EU1 pattern and its influence on surface temperatures. In the later semi-period the composite difference of winter HA_{500} is reminiscent of the NAO pattern instead, whose impact on snow cover is confined to western Eurasia (not shown).

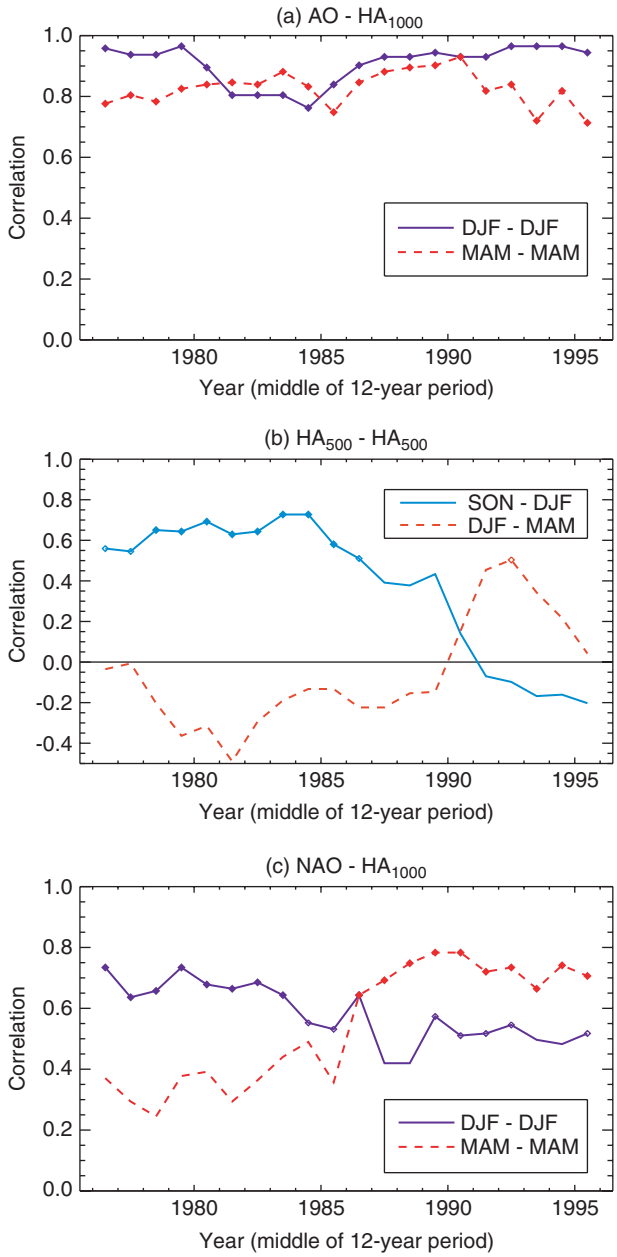

Figure 4. (a) Concurrent rank correlation between the AO and area-weighted geopotential height anomaly (HA) at 1000 hPa, HA_{1000}, in winter (solid) and spring (dashed). (b) As (a) except for HA at 500 hPa, HA_{500}. (c) As (a), except between the NAO and HA_{1000}. This figure is available in colour online at http://www.interscience.wiley.com/ijoc

Next, we discuss the strong winter–spring relation that emerged after the mid 1980s. Figure 4(c) shows the concurrent seasonal correlation between the NAO and HA_{1000} in winter and spring. The figure illustrates that the AO–NAO connection is strongest in the cold season in the earlier semi-period whereas the relation between the two in the spring is only significant after the mid 1980s. This difference in the warmer season connection may be due to the snow–atmosphere relation, which is found only in the later period. Spatial patterns of sea-level pressure associated with the March AO are shown in Figure 5(a) and (d). In the Atlantic sector, before the 1980s, the March AO pattern is limited to the North Atlantic basin, having little influence

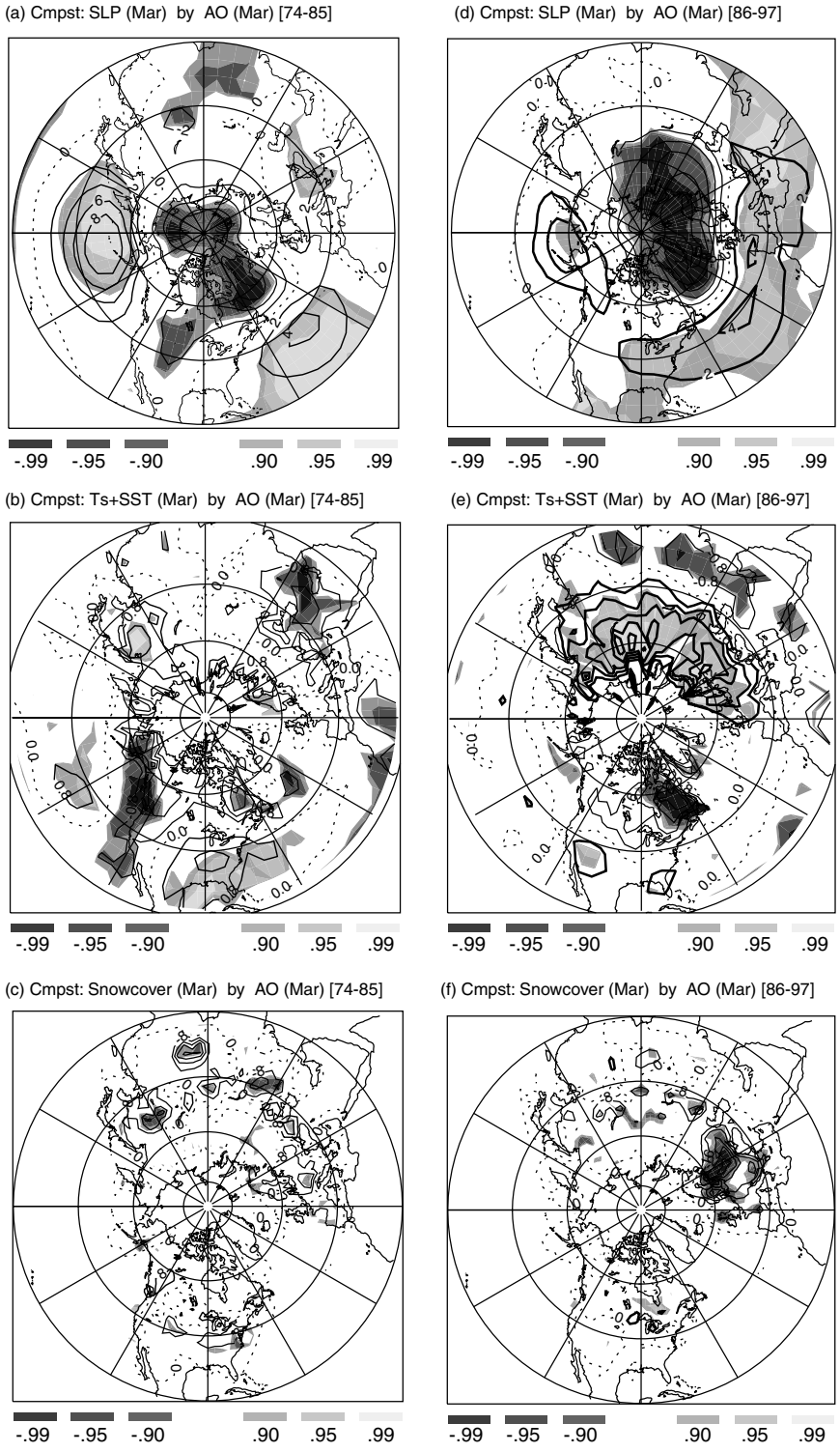

Figure 5. (a) Same as Figure 3(a) but for March sea-level pressure and the March AO. Contour interval is 2 hPa. (b) As (a), but for the combined March surface temperature over land (T_s) and ocean (SST). Contour interval is 0.8 K. (c) As (a), but for March snow cover. Contour interval is 8%. (d) As (a), (e) as (b) and (f) as (c), except for the period 1986–97

over Eurasia, whereas after the mid 1980s the March AO pattern extends into western Eurasia. This pattern is persistent, beginning in January in the later semi-period (not shown), and implies possible interaction between snow extent and the atmospheric circulation associated with the dominant mode variability from winter to spring.

Previous studies have established that the observed positive trend in the dominant mode is associated with the surface temperature T_s increase over the northern part of Eurasia, especially northern Europe and the Central Siberian Plateau (area around 100 °E; Hurrell and van Loon, 1997; Clark *et al*., 1999; Trigo *et al*., 2002). As expected from the difference in the spring AO pattern between the two semi-periods (Figure 5(a) and (d)), only for the later semi-period are significant areas of warm T_s (associated with the AO) observed over northern Eurasia, with the strongest signal over northeastern Europe (along 30 °E longitude) and the Central Siberian Plateau (Figure 5(b) and (e)). Consequently, a significant AO–snow-extent relation is only observed in the later semi-period. During the later period, snow-cover extent is mostly influenced over the area along 30 °E where snow-cover extent is sensitive to intraseasonal temperature variance (Figure 5(c) and (f)). The composite maps from January through to March produce substantially the same results, except for the gradual northeastward retreat of those areas of snow cover influenced by variability in the AO (not shown). The duration of the relation between the AO, T_s and snow cover is likely responsible for the significant winter AO–spring SNC_{EUR} relation depicted in Figure 2(b) for the later semi-period. Figure 6 summarizes schematically the changes described in seasonal relationships in the sub-decadal covariability between SNC_{EUR} and the AO before and after the mid 1980s.

Little is understood about snow–climate interactions that span from the warm to cold seasons; however, it most probably differs from those attributed to autumn SNC_{EUR} and the winter climate, since the troposphere

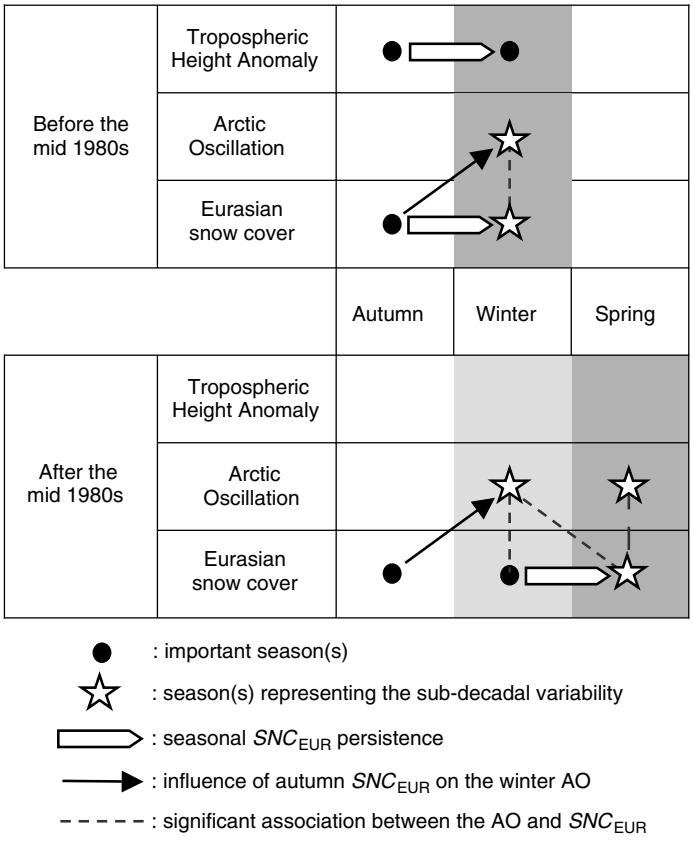

Figure 6. Schematic diagram of changes of the seasonal relationships in the sub-decadal covariability between Eurasian snow cover anomaly (SNC_{EUR}) and the AO. Dark (light) shading denotes strong (modest) concurrent relation between the AO and NAO

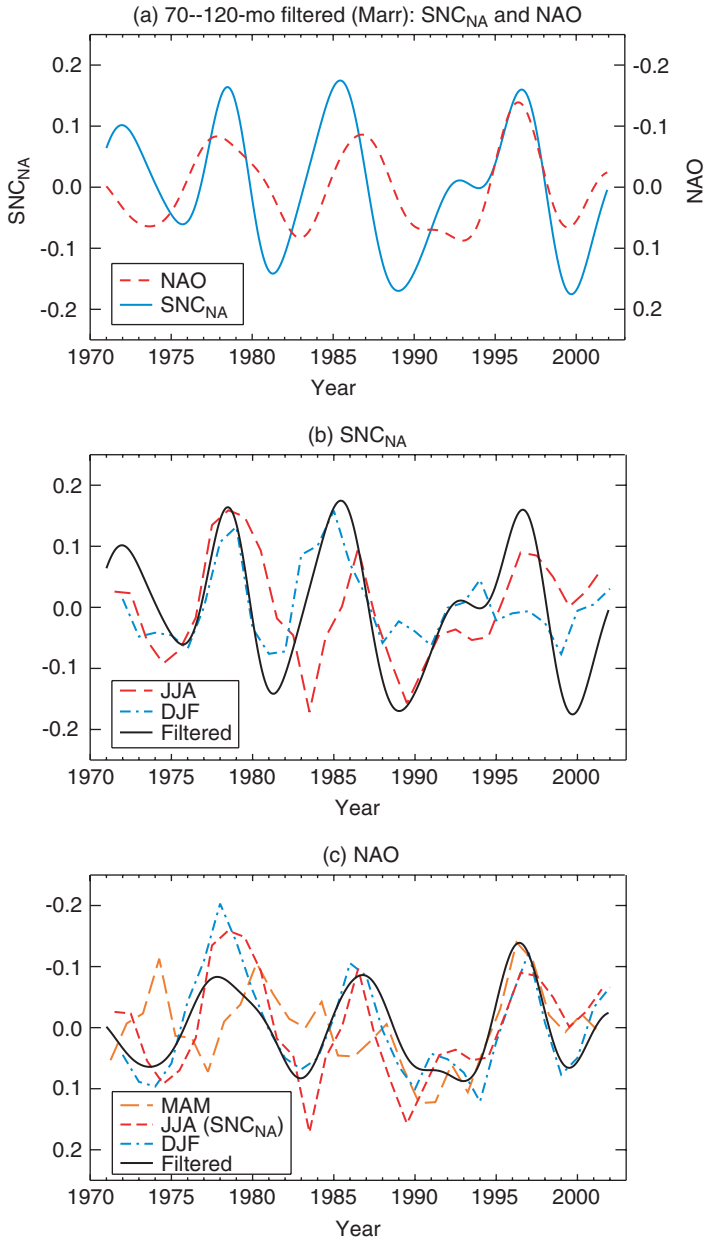

Figure 7. (a) As Figure 1(a), except for North American snow cover (solid; SNC_{NA}) and the NAO (dashed; scale at right). (b) As Figure 1(b), but for SNC_{NA}. (c) As (b), but for the NAO (thick) and its DJF (dash-dotted) and MAM (long-dashed) seasonal anomaly. JJA SNC_{NA} (dashed) is superimposed. This figure is available in colour online at http://www.interscience.wiley.com/ijoc

and stratosphere are uncoupled in the warm season. Instead, dynamical pathways are most probably confined to the lower troposphere. Also, no clear evidence was found in this study that snow cover anomalies influence the atmospheric circulation from winter to spring seasons.

Finally, we look at the sub-decadal variability of the NAO and its relation to the North American snow cover anomaly (SNC_{NA}) in Figure 7. The bandpass-filtered NAO and SNC_{NA} show two lead changes: the first in late 1970s and the second in the early 1990s (Figure 7(b)). In the first period, the NAO appears to lead, whereas in the second it lags. In the third period, the NAO leads slightly, but they vary mostly

in phase. Interannual variability of seasonal SNC_{NA} resembles that of SNC_{EUR}, in that winter SNC_{NA} dominates the interannual fluctuations in the earlier period but the warm season accounts for more of the sub-decadal variations in the later period. Concerning the NAO and SNC_{NA} covariability, the sub-decadal NAO variability (Figure 7(c)), which shares similar characteristics with respect to seasonal dependence as the AO (Figure 1(c)), is astonishingly well depicted by June to August (JJA) SNC_{NA} (short dashed line in Figure 7(c); cf. Figure 7(b)). This result suggests that JJA SNC_{NA} variability is closely related to the sub-decadal NAO variability, consistent with previous studies (Bamzai, 2002; Bojariu and Gimeno, 2003; Saito and Cohen, 2003; Saunders *et al*., 2003).

4. CONCLUSION

We attempt in this study to gain a deeper insight into the covariability between continental snow cover extent and the dominant mode of atmospheric variability, the AO or NAO, on sub-decadal time scales for the remotely sensed period. We found that there were changes in the structure of the covariability. A significant change occurred in the mid 1980s in the relation between SNC_{EUR} and the AO. Before the mid 1980s the autumn SNC_{EUR}–winter AO relation is considered to have been decisive in the sub-decadal covariability, with snow cover leading by several or more months. After the mid 1980s, loss of autumn–winter SNC_{EUR} persistence and the emergence of a strong AO–SNC_{EUR} connection from winter to spring brought about an in-phase relationship on sub-decadal time scales. For the NAO and SNC_{NA}, the bandpass-filtered series shows two lead changes in the late 1970s and early 1990s, but the sub-decadal variability of the NAO is closely related to that of summer SNC_{NA} throughout the remotely sensed period.

The entire period examined in this study did experience a long-term increase of high-latitude T_s and a decrease of continental snow-covered area (cf. figures 3 and 10 in Serreze *et al*. (2000)). Also, the length of the analysis period is limited. How these long-term trends may have also impacted the relationship between snow and the dominant mode of winter atmospheric variability was not explored in our study. It remains for further research to determine whether the change detected in the sub-decadal covariability between continental snow cover anomalies and atmospheric variability of hemispheric scale is due in part to a long-term increasing trend of high-latitude T_s and decreasing trend in snow-covered area in recent decades, or as part of internal inter-decadal fluctuations of the climate system. Well-organized general circulation model simulations and/or observational analysis of more extended length are required to answer this question.

ACKNOWLEDGMENTS

This investigation was partly supported by NSF grant ATM-0124904.

REFERENCES

Bamzai AS. 2002. Relationship of snow cover variability and Arctic oscillation index on a hierarchy of time scales. *International. Journal of Climatology* **23**: 131–142.

Barnston AG, Livezey RE. 1987. Classification, seasonality and persistence of low-frequency atmospheric circulation patterns. *Monthly Weather Review* **115**: 1083–1126.

Bojariu R, Gimeno L. 2003. The role of snow cover fluctuations in multiannual NAO persistence. *Geophysical Research Letters* **30**(4): DOI: 10.1029/2002GL015651.

Czaja A, Frankignoul C. 1999. Influence of the North Atlantic SST on the atmospheric circulation *Geophysical Research Letters* **26**: 2969–2972.

Clark MP, Serreze MC, Robinson DA. 1999. Atmospheric controls on Eurasian snow extent. *International Journal of Climatology* **19**: 27–40.

Cohen J, Entekhabi D. 1999. Eurasian snow cover variability and Northern Hemisphere climate predictability. *Geophysical Research Letters* **26**: 345–348.

Cohen J, Salstein D, Saito K. 2002. A dynamical framework to understand and predict the major Northern Hemisphere mode. *Geophysical Research Letters* **29**: DOI: 10.1029/2001GL014117.

Feldstein SB. 2002. The recent trend and variance increase of the annular mode. *Journal of Climate* **15**: 88–94.

Gong G, Entekhabi D, Cohen J. 2003. Modeled Northern Hemisphere winter climate response to realistic Siberian snow anomalies. *Journal of Climate* **16**: 3917–3931.

Hurrell JW, van Loon H. 1997. Decadal variations associated with the North Atlantic oscillation. *Climatic Change* **36**: 301–326.

Jones PD, Moberg A. 2003. Hemispheric and large-scale surface air temperature variations and an update to 2001. *Journal of Climate* **16**: 206–223.

Kalnay E, Kanamitsu M, Kistler R, Collins W, Deaven D, Gandin L, Iredell M, Saha S, White G, Woollen J, Zhu Y, Chelliah M, Ebisuzaki W, Higgins W, Janowiak J, Mo KC, Ropelewski C, Wang J, Leetmaa A, Reynolds R, Jenne R, Joseph D. 1996. The NCEP/NCAR 40-year reanalysis project. *Bulletin of the American Meteorological Society* **77**: 437–471.

Marshall J, Kushnir Y, Battisti D, Chang P, Czaja A, Dickson R, McCartney M, Saravanan R, Visbeck M. 2001. North Atlantic climate variability: phenomena, impacts and mechanisms. *International Journal of Climatology* **21**: 1863–1898.

Plumb A. 1985. On the three-dimensional propagation of stationary waves. *Journal of the Atmospheric Sciences* **42**: 217–229.

Rayner NA, Parker DE, Horton EB, Folland CK, Alexander LV, Rowell DP, Kent EC, Kaplan A. 2003. Global analysis of sea surface temperature, sea ice, and night marine air temperature since the late nineteenth century. *Journal of Geophysical Research: Atmosphere* **108**(D14): DOI: 10.1029/2002JD002670.

Robertson AW. 2001. Influence of ocean–atmosphere interaction on the Arctic Oscillation in two general circulation models. *Journal of Climate* **14**: 3240–3254.

Robinson DA, Dewey F, Heim Jr R. 1993. Northern Hemispheric snow cover: an update. *Bulletin of the American Meteorological Society* **74**: 1689–1696.

Saito K, Cohen J, Entekhabi D. 2001. Evolution of atmospheric response to early-season Eurasian snow cover anomalies. *Monthly Weather Review* **129**: 2746–2760.

Saito K, Cohen J. 2003. The potential role of snow cover in forcing interannual variability of the major Northern Hemisphere mode. *Geophysical Research Letters* **30**(6): DOI: 10.1029/2002GL016341.

Saunders MA, Qian B, Lloyd-Hughes B. 2003. Summer snow extent heralding of the winter North Atlantic oscillation. *Geophysical Research Letters* **30**(7): DOI: 10.1029/2002GL016832.

Serreze MC, Walsh JE, Chapin III FS, Osterkamp T, Dyurgerov M, Romanovsky V, Oechel WC, Morison J, Zhang T, Barry RG. 2000. Observational evidence of recent changes in the northern high-latitude environment. *Climatic Change* **46**: 159–207.

Thompson DW, Wallace JM. 1998. The Arctic oscillation signature in the wintertime geopotential height and temperature fields. *Geophysical Research Letters* **25**: 1297–1300.

Torrence C, Compo GP. 1998. A practical guide to wavelet analysis. *Bulletin of the American Meteorological Society* **79**: 61–78.

Trigo RM, Osborn TJ, Corte-Real JM. 2002. The North Atlantic oscillation influence on Europe: climate impacts and associated physical mechanism. *Climate Research* **20**: 9–17.

Wang J, Ikeda M. 2000. Arctic oscillation and Arctic sea-ice oscillation. *Geophysical Research Letters* **27**: 1287–1290.

Zhou S, Miller AJ, Wang J, Angell JK. 2002. Downward-propagating temperature anomalies in the preconditioned polar stratosphere. *Journal of Climate* **15**: 781–792.

